SP2018_117

Space Propulsion Conference 2018, Spain

DEVELOPMENT OF IGNITION UNIT FOR A LIQUID PULSED PLASMA THRUSTER

BARCELONA RENACIMIENTO HOTEL, SEVILLE, SPAIN / 14 – 18 MAY 2018

Cristian Dobranszki [(1)], Igor O. Golosnoy [(1)], Stephen B. Gabriel [(1)]

[(1)] *University of Southampton, B20 TDHVL, University of Southampton, University Road, Southampton, SO171BJ, United Kingdom*
Email: C.Dobranszki@soton.ac.uk; I.Golosnoy@soton.ac.uk; sbg2@soton.ac.uk

KEYWORDS:
Pulsed Plasma Thrusters (PPT), PFPE, Electrowetting Tip Ignition (ETI), Ignition Unit

ABSTRACT:
Solid-fed Pulsed Plasma Thrusters (PPTs) are the only mission employed devices to-date, although they suffer from low-efficiency and lifetime limiting post-ablation effects; oppositely, gas-fed PPTs offer high efficiency (~15 – 50 %) and no contamination; however, they are subject to propellant leakage issues, difficult ignition synchronisation and higher implementation costs. Liquid-fed PPTs require the sub-systems to be revisited to adapt the device to the intrinsic benefits of fluid propellants; it is suggested to use electrowetting to initiate Perfluoropolyether (PFPE) motion under the influence of electric fields. Employing a combination of dielectric materials, locally enhanced electric fields may be manipulated to decrease the ignition voltage and consequently increase efficiency. Preliminary measurements of PFPE bulk breakdown and the electrowetting-tip ignition at the liquid surface leading to reliable ignition voltages of 8.98 ± 0.86 kV are reported. The significance of PFPE motion at the cathode/vacuum interface is discussed and a vacuum breakdown mechanism relevant to the system is hypothesized, based on the MDV vacuum breakdown model.

NOMENCLATURE:

Symbol	Parameter
r_{tip}	Tip radius
d	Interelectrode distance
h_c	Cover height (from liquid level)
w_{ch}	Channel width
Λ_{PFPE}	Thickness of PFPE layer
R_c	Cover (inner) radius
r_c	Cathode radius
$R_{cab,sw}$	Resistance of cables and switch
t_R	Rise time – Leading edge
t_F	Fall time – Trailing edge
t_P	Pulse width (time)
H_s	Height at maximum saturation
h_0	Height of liquid level at rest
h_s	Height at partial saturation
v_{PFPE}	PFPE speed
τ_{trail}	Time constant of trailing edge
τ_{drop}	Time constant of drop segment
V_{ap}	Applied voltage
V_{ig}	Ignition voltage

1. INTRODUCTION

The motivation behind the development of Liquid-fed Pulsed Plasma Thruster (LPPT) ignition is based on a lack of operational system approach with the aim of improving Pulsed Plasma Thruster (PPT) efficiency and consequently industrial competitiveness. Sub-systems such as propellant storage, feeding and ignition require combined analysis to produce an optimised working device. The use of traditional spark plugs restricts the design of LPPTs, since the liquid is often localised at some distance from the main electrodes, subjecting the spark plug to spatial constraints. Moreover, the fluidity of the liquid propellants offers an avenue of novel design possibilities in terms of propellant storage, facilitating the diverse thrust arrangement requirements for nanosatellites and cubesat systems, by removing the otherwise fixed volume occupied by the PTFE propellant bar. Furthermore, Solid-fed Pulse Plasma Thruster (SPPT) ablation rate can only be controlled via the delivered energy of the main discharge, unavoidably leading to symmetry loss (canting) after numerous ablations [1] and failure via carbon deposition resulting in short circuiting [2]. In contrast, Gas-fed Pulsed Plasma Thrusters (GPPTs) and LPPTs offer reduced late-time ablation effects [3] and carbon deposition [4], and accurate dosing of the propellant [5], resulting in an extended lifetime.

LPPTs have been shown to overcome propellant charring [4], a major drawbacks of SPPTs; additionally, they can offer low-cost configurations for fuel feeding, which increases electrical efficiency compared to fast-acting valves currently predominating gas- and liquid-fed devices, such as capillary effects [3, 5], porous media propellant delivery [6] – also referred to as Passive Flow Control (PFC) unit – or a combination of both [4].

The propellant of choice is Perfluoropolyether (PFPE), a chemically stable and non-volatile lubricant, achieving similar performance to the long-standing PTFE [7] – the commercially available Fomblin Y LVAC 25/6, produced by Solvay [8] is used throughout these experiments – the density, vapour pressure and surface tension of this material are 1.9×10^{3} kg/m^{3}, 8×10^{-8} mbar and 22 dyne/cm [8]. However, many important aspects of PFPE operation have not been investigated, such as ignition reliability of the bulk or over the surface in vacuum conditions and liquid motion under electric fields which has the potential to form a new and energetically cheap propellant feeding method.

It is suggested to use electrowetting to initiate PFPE motion under the influence of electric fields. Moreover, while PFPE exhibits motion towards the region of low potential, it fills small gaps next to the spark electrode, increasing the local field, which in-turn lowers the breakdown voltage. The proposed ignition system uses an auxiliary electrode, designed to increase the electric field next to the needle-shaped electrode placed in the dielectric cover. Negative applied voltage at the cathode drives the liquid towards the gap between the needle and the cover, achieving breakdown at reduced voltages. The drawback of the Electrowetting Tip Ignition (ETI) are the time-delay introduced between switching the ignition voltage and breakdown, and the liquid trapped in the capillary (between cathode and cover). The PFPE liquid motion, which is inferred to lead to ignition, is shown to be controlled by varying the electric field.

Finally, the electrowetting is suggested as a novel concept for LPPTs, removing the need of fast-acting valves or moving parts, since the wetting properties can be controlled by external electric fields. The design for the feeding system depends on the wetting characteristics of PFPE on different surfaces.

2. IGNITION UNIT DESIGN

2.1. Operation Principle

The conceptualised operating principle of this ignition unit relies on the locally enhanced electric field at the surface of the cathode. The electric field enhancement is driven by the dielectric and wetting properties of PFPE. The ignition sequence requires PFPE to be in contact with the cathode. The voltage applied to the cathode (negative polarity), initiates PFPE movement, effectively coating the cathode surface with a visible layer of the dielectric liquid. As a result, the dielectric properties of the layer enhance the electric field locally which initiates electron extraction form the cathode surface, consequently leading to surface discharge.

2.2. Geometry, Materials and Dimensions

Fig. 1 depicts a schematic of the test cell used in all experimental measurements. In order to investigate the viability of the bulk discharge in PFPE, a quartz dielectric cover is placed over the tungsten cathode. Both are partially immersed in liquid; with the cathode tip (radius at the tip of r_{tip} = 157.03 ± 5.67 µm obtained by diamond polishing) advanced beyond the cover height at least 2 mm (to avoid electric field shielding). The anode is fully submersed in PFPE forming a 1.5 mm gap in a point-to-plane configuration (fig. 1a) – the discharge is forced to take place only within the liquid bulk.

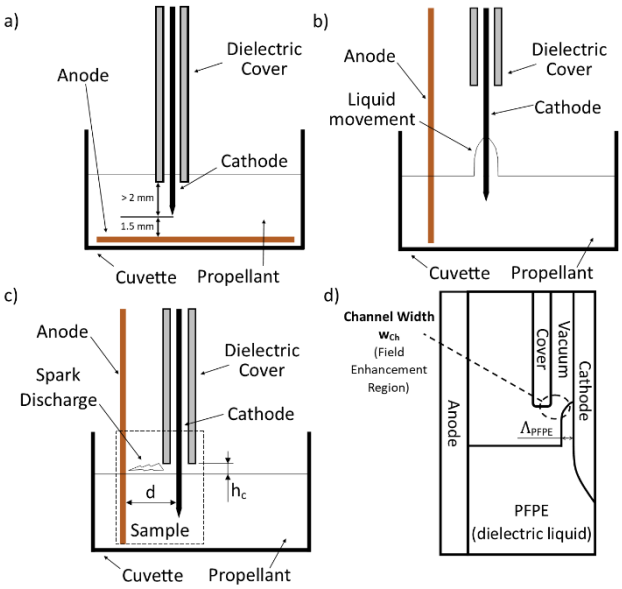

Figure 1. Cross-sectional representation of the experimental setups – anode is grounded. a) PFPE bulk breakdown under impulse conditions, in a high vacuum of 10^{-6} mbar; b) Liquid movement over the cathode surface under an applied electric field; c) Surface flashover and electric field enhancement using liquid flow; d) Schematic of the liquid motion at the cathode surface, showing rise of PFPE layer (thickness Λ_{PFPE}) and the electric field enhanced channel, w_{ch}.

The propellant advancing speed at the cathode surface is measured using the parallel electrode setup schematic shown in fig. 1b. Finally, fig. 1c and 1d correspond to the ignition tests wherein the

PFPE propellant movement influenced by the applied electric field is employed to reduce the ignition voltage (voltage required to produce surface flashover). The parallel arrangement, with an interelectrode distance of d = 1.233 ± 0.064 mm and cover height of h_c = 1.335 ± 0.038 mm, is used in order to allow liquid movement to enhance the local electric field at the cathode surface, initiating surface discharge at reduced voltages.

A lanthanated tungsten (WLa1.5) cylindrical rod (r_c = 0.499 ± 0.006 mm) is used as cathode. The lanthanum doping lowers the work function and facilitates electron extraction while maintaining a high melting temperature. Additionally, the oleophilic behaviour of PFPE on the cathode surface exhibits favourable wetting properties. The quartz dielectric cover ε_{quartz} = 3.80 [9] ensures the breakdown is located in the vicinity of the liquid surface. The thick quartz cover walls determine the minimum interelectrode distance achievable in the setup and the cover inner radius of R_c = 0.979 ± 0.039 mm does not restrict the liquid flow in the cover-cathode void – potentially enhancing the electric field at the closing channel width, w_{ch} (fig. 1d). Quartz has been selected as the dielectric cover due to its transparency, allowing observations of the liquid behaviour in the cover-cathode void. The anode is a 2 mm thick and 5 mm wide slab – copper has been selected to simplify integration of the ignition unit with the thrust chamber electrodes; copper has been previously observed to offer successful results as PPT electrodes [2]. The cuvette holding the PFPE fluid is a transparent borosilicate beaker. In the early stages of these experiments alumina was used as cuvette and cover.

2.3. Electrical Circuit

The circuit employed for LPPT ignition is shown in fig. 2. This setup has been implemented to simulate the PPT circuitry, control the energy delivered from shot to shot (via a capacitor stored energy) and to create reproducible conditions in terms of the applied voltage and hence the electric field, which has been observed to influence the liquid movement.

In the PPT circuit, a two-stage sequence is employed: the ignition stage and the thrusting stage. There is an overlap of the two stages, since charge carriers created by the ignition stage act as seeds for the thrusting discharge (and thrusting stage). Therefore, the integration of the thrusting circuit relies heavily upon the ignition unit; which has been considered when designing the ignition unit circuit in fig. 2.

The high voltage Power Supply Unit (PSU) is manually controlled and current limited to 2.4 mA. It has a maximum rise time of 100 ms, repeatability within 0.1% and a ripple of less than 0.03% RMS, as rated by the manufacturer. The low voltage PSU is current limited to 100 mA and voltage limited to 25 V. this provides a consistent step function signal to the switching coil (hence applying the same magnetic force to the metal contacts).

Data collection consists of a semi-automated system, the oscilloscope is LabVIEW controlled using the PC. As discharge is recorded by the voltage probe and oscilloscope, the PC calls the data and stores it.

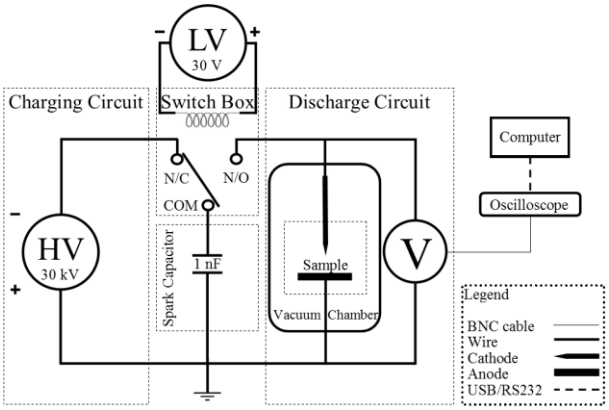

Figure 2. Circuit employed for ignition of PFPE-fed liquid pulsed plasma thruster.

The circuit resistance, including the mechanical switch contact resistance was measured using a low resistance ohmmeter ($R_{cab,sw}$ = 17.7 ± 0.01 mΩ). Critical phenomena related to the circuit are the mechanical switch and the PFPE movement. The double-pole-double-throw mechanical switch comprises of metallic contacts inside a vacuum enclosure, magnetically operated using a coil. Due to its construction, transient effects such as arcing and contact bouncing occur between the contacts; this introduces additional time dependent resistance, inductance and capacitance in the circuit resulting in jitter, voltage flyback and increased noise. Arcing within the switch establishes an electrical connection between the two terminals prior to the mechanical contact, gradually increasing the voltage on the cathode (prior to the full voltage being applied). Consequently, PFPE movement is enabled at an earlier stage than expected. The dielectric liquid wetting the cathode surface varies the gap capacitance, effectively creating a double layer capacitor (vacuum and PFPE).

Additionally, discharges between the cathode and anode may increase the surface roughness (ablation) through electrode erosion – affecting the liquid motion over the cathode surface. Surface analysis of the cathode using measurements techniques such as XPS has not been performed after testing. However, carbon deposition due to electrode ablation is a well-known issue within vacuum technology [10, 11] and it is considered as a possible limitation in the experimental design.

3. PRELIMINARY RESULTS

3.1. Bulk Discharge

By means of the setup presented in fig. 1a and the electrical setup of fig. 2, the bulk breakdown threshold within PFPE is measured under a diverging electric field (point-to-plane). The voltage is increased in steps of 0.5 kV/test, until the desired test voltage is reached; each measurement is repeated five times. The manufacturer rated breakdown field is 15.7 kV/mm [12]. The PFPE sample will be investigated under electric fields of 37.5 MV/m resulting from an applied voltage of up to -12 kV; SPPT ignition can be reliably achieved at voltage magnitudes of 12 kV [13], the ignition voltage of PFPE is of interest – from a competitive perspective – below this value.

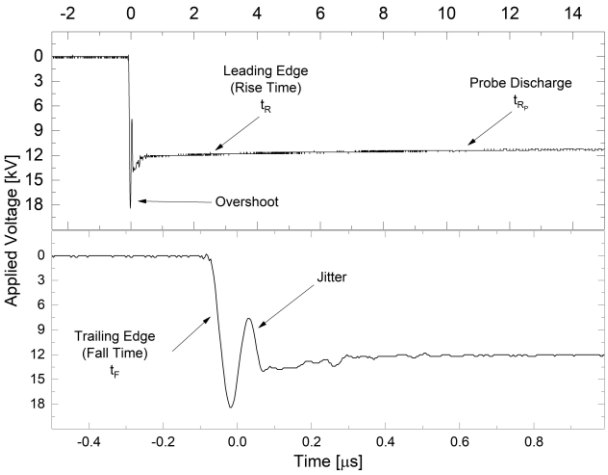

Figure 3. PFPE bulk breakdown test waveform under a point-plane arrangement with interelectrode gap of 1.5 mm and -12 kV applied voltage at the cathode.

No discharge was observed for bulk breakdown tests as shown in fig. 3. This indicates that bulk discharge of PFPE, with the aim of charge carrier generation to initiate the main discharge is futile in the ignition voltage range appropriate to PPTs.

The short fall time in fig. 3 represents the charging of the sample capacitance. However, in the point-to-plane arrangement, the capacitance is negligible giving a fall time of 22.08 ns (measured between 10 and 90% of the test voltage – excluding overshoot).

3.2. PFPE Liquid Motion

Measurements of the PFPE wetting properties have been performed using the setup presented in fig. 1b and with a modified electrical setup, presented in fig. 4.

The mechanical switch is eliminated in the electrical setup of fig. 4 to avoid any transient RLC effects (such as jitter and flyback voltage), yielding a repeatable voltage ramp-up at the cathode and ensuring consistency throughout the PFPE rise measurements. The high-speed camera is used to capture the height achieved by the fluid for various applied voltages. Each image has been captured 20 seconds after the voltage was applied to the cathode to ensure the liquid rise reached the maximum saturation height, H_s. The proportionality between the applied voltage and the PFPE height increase is evident from fig. 5.

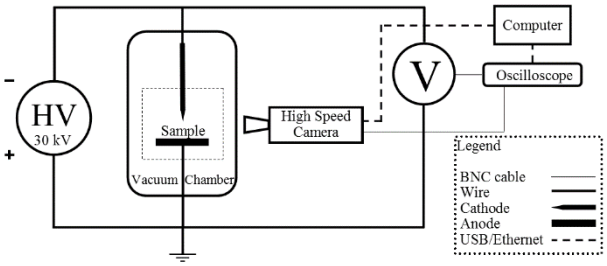

Figure 4. Electrical diagram of the PFPE liquid rise experiments – the associated test cell is represented in fig. 1b. The high-speed photography was set for an exposure time of 353 μs.

The liquid motion observed inside the vacuum chamber is governed by the dynamic depicted in fig. 5. The liquid dielectric moves against gravity under the influence of the electric field; effectively coating the cathode surface with a visibly discernible PFPE layer, Λ_{PFPE}. As voltage is increased, the PFPE layer is observed to grow in height above the liquid surface level, h_0. Partial saturation levels, h_s arise at various levels as the liquid coating increases in height. These are observed as the liquid tendends to extend over the interelectrode gap – bridge formation (shown in fig. 6). The PFPE layer increases in thickness when bridges collapse back into the liquid layer.

To simulate the conditions used in the ignition tests the electrical setup of fig. 2 is introduced again for the PFPE speed measurements. The PFPE liquid motion against gravity is captured using the high-speed camera – under an impulse voltage of −13 kV. The camera records until a discharge occurs, which ensures the entire liquid movement is captured.

The liquid height measurement is performed using the software ImageJ. Scale calibrations are individually done (using the well-defined cathode diameter of 0.998 ±0.011 mm). A measurement is taken between the cuvette edge (which represents the reference value) and the peak of the PFPE layer at the surface of the cathode – effectively, measuring the length of the PFPE/metal interface

oriented towards the interelectrode region. Each data point consists of 5 measurements and the corresponding standard deviation of the statistical sample is calculated.

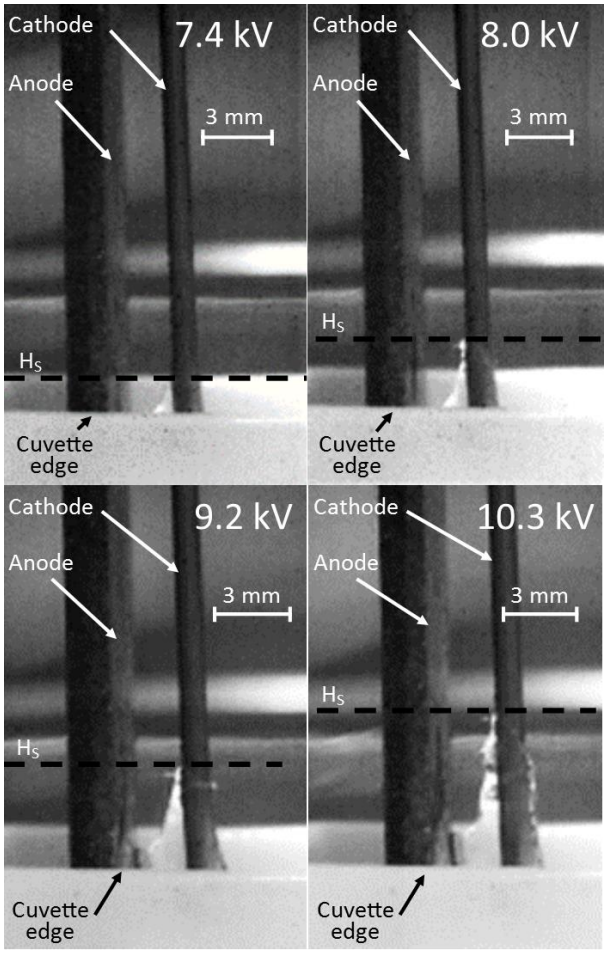

Figure 5. PFPE fluid movement over the surface of the cathode. The liquid saturation height, H_s increases as voltage is increased. Image contrast enhanced using Photoshop. Note: the scale bars are not equivalent between images.

Partial saturation levels are reached as the liquid attempts to bridge over the gap between the electrodes during its rise. These structures can be readily determined, and not surprisingly they map the skewed data points in the trend of fig. 6. Linear regression fitted to the data in fig. 6, resembles a velocity of $v_{PFPE} = (2.42 \pm 0.10) \times 10^{-4}$ mm/μs, with a corresponding value of χ^2=0.96, suggesting that the standard linear equation fits the data reliably, as expected. Field enhancement due to liquid rise occurs prior to the maximum saturation level, H_s (where liquid growth speed is expected to drastically decrease $v_{PFPE} \rightarrow 0$); hence, the relevant section of the liquid growth speed is the initial section, prior to maximum saturation.

Qualitative and quantitative observations of the liquid under the influence of electric fields confirms that the applied voltage (and resulting electric field) is directly proportional with the height saturation level, H_s in the studied timeframe of 20 s per applied voltage.

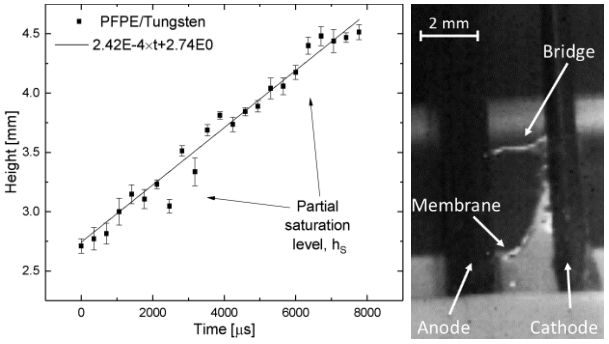

Figure 6. PFPE motion under an applied voltage (impulse) of -13 kV. (Left) Liquid motion coating the cathode surface, as a function of time; (Right) Image of membrane and bridge structure at 11.7 ms – continuation of the plot.

Furthermore, it is hypothesized that the electric field components at the cathode surface may be responsible for the liquid motion. The tendency of the electric field to coat the cathode surface and its tendency to form bridges across the interelectrode gap may be driven by the tangential and normal electric field components at the cathode surface, respectively. More data is required to conclude.

3.3. Surface Breakdown Ignition

The electrical circuit in fig. 2 and the setup in fig. 1c have been employed to measure the ignition voltage of the propellant under the influence of its motion. A typical pulse waveform corresponding to an applied voltage of V_{ap}= −11 kV is shown in fig. 7. The luminescent arc discharge occurs prior to the voltage at the cathode reaching V_{ap}; the measured arc discharge voltage is considered as ignition voltage, V_{ig}.

The pulse width is annotated by t_P and measures the time elapsed between 90% of the trailing edge voltage and 10% of the leading edge voltage; hence, the time between the end of the fall time and beginning of the rise time. The fall time, t_F and pulse width, t_P define the pre-discharge time.

The extended trailing edge in fig. 7a is expected due to the large capacitance formed between the sample and electrodes. This may be reduced by decreasing the immersion depth of the cathode and the cathode-anode length separated by the dielectric cover. Since the sample capacitance is significant, this may be calculated by finding the characteristic time constant of the trailing edge. The liquid motion over the cathode surface varies the

time constant of the liquid/vacuum gap. The time constant of the two transient times in fig. 7b are τ_{trail} = 104.9 ± 0.3 µs and τ_{drop} = 58.4 ± 4.4 ns showing a substantial drop in in the RC value.

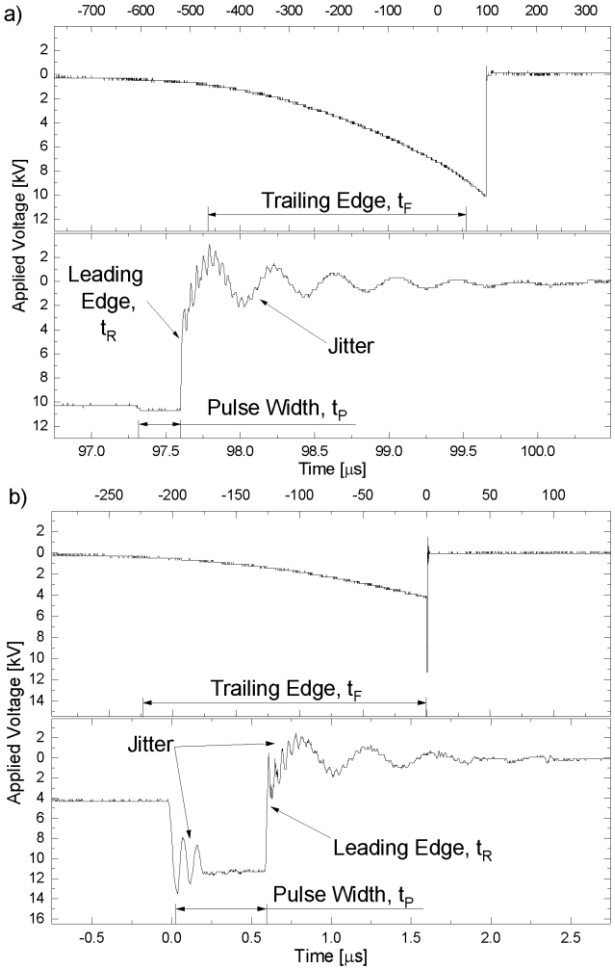

Figure 7. Sample waveforms of ignition tests using PFPE in vacuum of 10^{-6} mbar with liquid movement and electric field enhancement at V_{ap} = −11 kV. a) Waveform of regular pulse. b) Waveform of irregular pulse with chopped trailing edge and 23% overshoot.

The low frequency-high amplitude jitter captured in fig. 3 and fig. 7 is an effect produced by the imbalance of (R/2L) < (1/√LC) which presumes underdamping conditions of the system. The high frequency-low amplitude jitter tracing the voltage signal is an effect specific to stray inductance, caused by the long cables involved (~150 cm total). The flyback voltage in the system, producing a considerable overshoot, is associated with the sudden change in current due to the cut-off (switching), namely V=L×(*d*i/*d*t).

In the data set measuring ignition voltage, 42 measurements have been taken, 4 of these show a sudden drop in the trailing edge (irregular pulse). Whether the drop in voltage is due to the mechanical switch (internal arcing causing electrical contact between terminals prior to mechanical contact) or a sudden change in the liquid dynamic at the cathode surface (effectively varying the capacitance) was not determined yet; however, assuming that the liquid dynamic is at fault, the operation of the ignition unit may need reconsidering to ensure this effect does not lead to failure or misfiring events. This is presently under investigation.

3.4. Discharge Reliability

The breakdown tests of the impulse voltage system under high vacuum (10^{-6} mbar) is presented in fig. 8; wherein the Weibull statistics yield an average breakdown value of V_{ig} = −8.98 ± 0.86 kV. The measurements are consecutive, with a 20 second rest time between each attempt. No misfiring was recorded throughout testing.

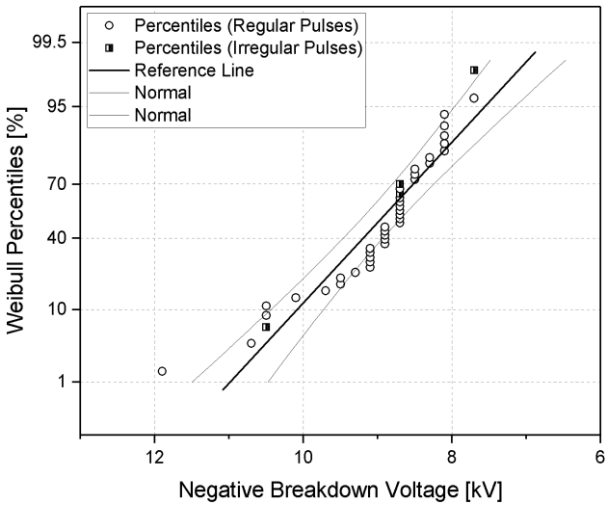

Figure 8. Two-parameter Weibull distribution of ignition testing; nominal ignition voltage V_{ig} = −8.98 kV, scale factor α = 121.895, shape factor β = 26.641 and 90% confidence band.

The associated electric field in front of the growing PFPE layer and at the electrode tip are 12 MV/m and 25 MV/m respectively, considering a measured Λ_{PFPE} = 200 µm and height of only h_s = 169 µm (based on a 700 µs pre-discharge time and the measured PFPE speed), i.e. without having formed the channel width, w_{ch} highlighted in fig. 1d.

The discharge reliability of this ignition unit prototype is demonstrated by the favourable preliminary statistics regarding its operation.

4. BREAKDOWN MECHANISM

Based on the experimental evidence – the measured PFPE velocity and breakdown voltage, the strong arc luminesces, computed electric field and since vacuum breakdown has not been obtained at such low electric fields without dielectric materials involved [11, 14], it follows that the breakdown mechanism must rely on the contribution of the PFPE dielectric layer.

The Metal Dielectric Vacuum (MDV) model proposed in [15] is most relevant within the electric field range of 10 – 20 MV/m [11, 16]. The mechanism of electron extraction leading to breakdown of the vacuum gap has not been conclusively established. However, it is proposed by Latham et al. to be based on thermionic emission – wherein the electric field penetrating the carbon (semiconductor) inclusion at the cathode surface enables the energy bands to bend, supplying sufficient energy to the electrons in the metal to overcome the Schottky barrier [17]; electron injection in the semiconductor produce heating and form a (conductive) electron channel [15] which initiates the thermionic emission from the metal surface [17] leading to discharge. There are several similarities between the observed phenomena and the MDV model; most important is the analogy of a streamer inside the PFPE layer with the hot electron channel inside the semiconductor inclusion. The electrowetting effect observed contributes to the bending of the energy bands [18]; additionally, electron injection due to the build-up charge at the metal/insulator junction has been demonstrated [19]. As electrons are injected, the dielectric layer is heated locally, and it may initiate vaporisation and bubble formation, consequently leading to streamers. Furthermore, electric field ionisation (field desorption) has been shown to be the dominating mechanism for vapour formation in dielectric liquids [20, 21], leading to streamer breakdown. It follows that the trapped space charge at the cathode surface and the induced electric field ionisation in the PFPE layer coating the cathode surface may both contribute to the streamer formation; which, via thermionic emission, can extract electrons and initiate ignition via breakdown – according to the MDV model.

It is evident that an arc discharge must involve more than electrons (FN field emission) due to the emitted light (in visible spectrum); however, the effect of electron bombardment of the anode (from a hot electron channel) may contribute significantly to the arc formation since the anode ablation has been experimentally observed in such systems [17]. Moreover, the presence of the liquid coating may protect the cathode from ablative back-scattering effects originated at the anode, extending the cathode lifetime in LPPTs.

The experiments conducted up to this point are insufficient to conclude upon a model for the breakdown mechanism. However, the MDV model proposed by Latham et al. [15] is the one supported by most theoretical and experimental evidence.

5. CONCLUSION

Preliminary tests of the wetting properties of PFPE under the influence of electric fields have been performed in high vacuum (10^{-6} mbar). It has been observed that PFPE exhibits motion against gravity with a bias towards the region of low electric field. The measured PFPE speed at the surface of the cathode is $(2.42 \pm 0.10) \times 10^{-4}$ mm/μs. The features of PFPE liquid motion are promising elements to explore for a capillary based PFPE feeding system. Considering the responsive motion of PFPE to applied electric fields, a feeding system using the resulting electric field from the ignition voltage is envisioned – eliminating the need of valves or PFC units and increasing PFPE efficiency. The use of PFPE electric field manipulation may be useful within the framework of PFCs, in order to enhance the surface wetting of the porous ceramic units, for example.

The discharge reliability of the ignition system proposed is evident from the favourable statistics, the short time prior to discharge does not prove to be a limiting factor for the operation frequency range of PPTs. The ignition voltage leading to breakdown of PFPE over the surface has been established at -8.98 ± 0.86 kV, which is within the operating regime for PPTs. The bulk discharge value of PFPE has been established to be above the measured threshold of -12 kV under a 1.5 mm point-plane gap and high vacuum conditions.

Future considerations are to decrease the ignition voltage required via the electrowetting-tip ignition method, ultimately making LPPTs more attractive to industry.

6. ACKNOWLEDGEMENTS

The authors would like to extend their appreciation to the EPSRC fund which financial supportes this work and to the efforts of the University of Southampton TDHVL staff who have greatly contributed to the experimental setup and results.

7. REFERENCES

1. Markusic, T.E. and Choueiri E.Y., *Visualization of Current Sheet Canting in a Pulsed Plasma Accelerator*, in *IEPC*. 1999, AIAA: Japan.
2. Ciaralli S., Coletti M. and Gabriel S.B., *Performance and lifetime testing of a pulsed plasma thruster for Cubesat applications.* Aerospace Science and Technology, 2015. **47**: p. 291-298.
3. Szelecka A. et al., *Liquid micro pulsed plasma thruster.* Nukleonika, 2015. **60**(2): p. 257-261.
4. Ling W., Schönherr T. and Koizumi H., *Characteristics of a non-volatile liquid propellant in liquid-fed ablative pulsed plasma thrusters.* Journal of Applied Physics, 2017. **121**(7): p. 073301.
5. Barral S. et al., *Development Status of an Open Capillary Pulsed Plasma Thruster with Non-Volatile Liquid Propellant*, in *IEPC*. 2013: Washington USA.
6. Scharlemann C. A., *Investigation of Thrust Mechanisms in a Water Fed Pulsed Plasma Thruster*, in *Aeronautical and Astronautical Engineering*. 2003, The Ohio State University: Ohio, USA.
7. Barral S., Kurzyna J. and Szelecka A. et al., *First Experimental Characterization of a Pulsed Plasma Thruster with Non-Volatile Liquid Propellant*, in *Space Propulsion Conference*. 2014: Germany.
8. KJLC (Kurt J Lesker Company). *Fomblin Y LVAC Vacuum Pump Oil*. 2013 [cited 09/04/2018] Available from: https://www.lesker.com/newweb/fluids/pdf/11-013-fl-ds-fombliny-datasheet-lvac-vacuumpumpoil.pdf.
9. Pillai A.S. and Hackam R., *Surface flashover of solid insulators in atmospheric air and in vacuum.* Journal of Applied Physics, 1985. **58**(1): p. 146-153.
10. Boxman R. L., Sanders D. M. and Martin P. J., *Handbook of Vacuum Arc Science & Technology: Fundamentals and Applications*. 1st ed. 1995, USA: William Andrew. p. 637-638.
11. Athwal C. S. and Latham R. V., *Switching and other nonlinear phenomena associated with prebreakdown electron emission currents.* J. Phys. D: Appl. Phys., 1984. **17**: p. 1029-1043.
12. Boccaletti G., *PFPE - Fomblin YVAC 25/6 Properties*, Personal communications with C. Dobranszki, Solvay 2017.
13. Ciaralli S., *A Study of the Lifetime of Miniaturized Ablative Pulsed Plasma Thrusters*, in *ECS*. 2014, Univeristy of Southampton.
14. Davies D.K. and Biondi M.A., *Vacuum Electrical Breakdown between Plane-Parallel Copper Electrodes.* Journal of Applied Physics, 1966. **37**(8): p. 2969-2977.
15. Latham R. V., Bayliss K. H., and Cox B. M., *Spatially correlated breakdown events initiated by field electron emission in vacuum and high-pressure SF6.* J. Phys. D: Appl. Phys., 1986. **19**: p. 219-231.
16. Cade N.A. and Latham R. V. et al., *Field-induced electron emission through Langmuir-Blodgett multilayers.* J. Phys. D: Appl. Phys., 1988. **21**: p. 148-153.
17. Athwal C. S. et al., *Field-Induced Electron Emission from Artificially Produced Carbon Sites on Broad-Area Copper and Niobium Electrodes.* IEEE Transactions on Plasma Science, 1985. **PS-13**(5): p. 226-229.
18. Arscott S. and Gaudet M., *Electrowetting at a liquid metal-semiconductor junction*. Applied Physics Letters, 2013 **103**, 074104
19. Matsui K. et al., *Space Charge Behavior in Low-density Polyethylene at Pre-breakdown.* IEEE Transactions on Dielectrics and Electrical Insulation, 2005. **12**(3): p. 406 - 415.
20. Hwang J.G. and Zahn M., *Mechanisms behind positive streamers and their distinct propagation modes in transformer oil.* IEEE Transactions on Dielectrics and Electrical Insulation, 2012. **19**(1): p. 162-174.
21. Davari N. et al., *Field-dependent molecular ionization and excitation energies: Implications for electrically insulating liquids.* AIP Advances, 2014. **4**(3): p. 037117.